

## **Hollow Optical Conduits for Vibrational Spectroscopy**

**Walter M. Doyle**  
**Axiom Analytical, Inc.**

### **Introduction:**

This article is concerned with the transmission of infrared radiation from a broadband thermal source -- typically modulated by a scanning Michelson interferometer -- to a measurement point and then to an infrared detector, most often located near the source. In these days of long distance fiber-optic telecommunication, it might seem that optical transmission is hardly a subject for discussion. However, practical optical fibers are not available for use at wavelengths much greater than 2.2  $\mu\text{m}$ , and all of the fundamental bands of organic molecules fall at these longer wavelengths. We thus must fall back on less elegant means of signal transmission if we wish to apply mid-infrared spectroscopy to situations in which the sample cannot conveniently be brought to the spectrometer.

Incoherent mid-infrared radiation can be transmitted between two points either by an imaging system or by a system of hollow conduits, or "lightguides". In the former approach, a combination of optical elements such as refracting lenses or aspheric reflectors is used to superimpose an image of the radiation source on the infrared detector. An example would be an open path air monitoring system, in which a telescope is used to form the radiation from the source into a nominally collimated beam and a second telescope is used to collect as much of this beam as possible and focus it on the detector. Transmission by this approach is limited by the inherent beam divergence resulting from the finite size of both the source and the transmitting optics. This effect can be mitigated to an extent by

using a series of optical elements to create intermediate images at various points along the optical path. (Ref. 1)

In the lightguide approach, the source radiation is again formed into a nominally collimated beam. However, in this case, the beam diameter is matched to the diameter of a reflecting lightguide, which serves to prevent further divergence of the beam while preserving the distribution of ray angles relative to the system axis. One can think of a uniformly illuminated lightguide as transmitting an optical signal from one end to the other without altering the geometric distribution of individual rays. An optical fiber is an example of an optical conduit in which the theoretically perfect internal reflection in a material such as fused silica is used to transmit radiation with extremely high efficiency. The mid-infrared optical fibers developed to date have not exhibited the degree of transparency and robustness required for most applications (Ref. 2). For applications requiring transmission more one or two meters, we are thus forced to use external reflection at the surface of either a metallic or a dielectric material. And while external reflectance can be quite high, especially near grazing incidence, it never reaches the theoretically perfect condition achievable with internal reflection. Maximizing transmission through a system of lightguides thus requires minimizing the number of wall reflections and restricting these reflections to angles, which are as close as possible to 90°. (grazing incidence). (Ref. 3)

In the discussion, below, I will use the ray-trace approach to analyzing the

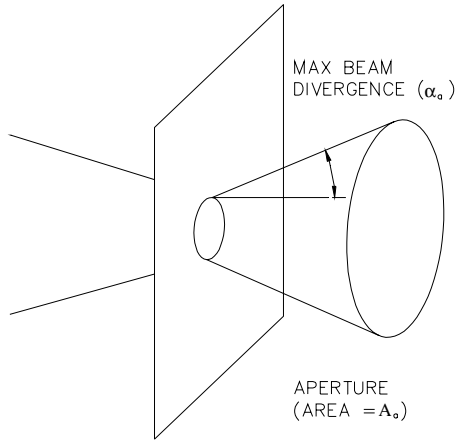


**Figure 1. Illustration of throughput for a uniformly illuminated circular aperture.**

performance of systems of lightguides. This is in contrast to the mode analysis approach often used in discussing optical fibers. However, it is appropriate in our case since the dimensions of the hollow lightguides are far greater than the wavelength of the optical radiation being conveyed. (Ref. 4)

### Throughput Considerations:

Throughput (also known as étendue) is a measure of the ability of an optical system to transmit power obtained from an incoherent source. A throughput value can be calculated at any element of the system – such as at a lens, detector surface, or interferometer aperture – where the radiation is uniformly distributed over an area and a range of angles. (Ref. 5) For a given aperture in an optical system, the throughput is defined by the equation. (Ref. 6)

$$\tau = \int_0^{\alpha_a} \cos \alpha \, d\Omega \, dA$$

where  $d\Omega = \sin \alpha \, d\alpha \, d\phi$

Here,  $\alpha$  is the angle between the direction of a given ray and the axis of the system and  $\phi$  is an azimuthal angle.

For a cone of radiation centered on the system axis, this becomes

$$\tau_a = \pi A_a \sin^2 \alpha_a$$

where  $A_a$  is the area of the aperture, and  $\alpha_a$  is the maximum divergence angle of radiation passing through the aperture. (See Figure 1.)  $\sin \alpha_a$  is often referred to as the numerical aperture (NA) of the device.

The “conservation of throughput” principle states that the throughput of an optical system can be no greater than the lowest throughput of any aperture in the system. For an extended radiation source, the total power transmitted through an optical system will be approximately proportional to this limiting throughput multiplied by the optical transmission for radiation traveling along the system axis. The conservation of throughput principle allows us to most effectively optimize the performance of an optical system by matching the throughputs of its various components to the limiting throughput. It also provides a simple way of determining the distribution of ray angles in various parts of the system. This is quite useful in estimating the performance of lightguides used in vibrational spectroscopy.

### Theoretical Basis for Approximating Lightguide Transmission Characteristics.

Practical lightguide systems used in vibrational spectroscopy generally employ straight, circular cross-section lightguides in conjunction with various mirror assemblies to couple between these and other optical components or between light guides of different orientations or diameters (Ref. 7). We thus will only consider straight lightguides here. The properties of bent lightguides have been discussed by Morhaim, et. al., and others. (Refs. 4,8)

To determine the transmission of a lightguide for a ray propagating at a specific

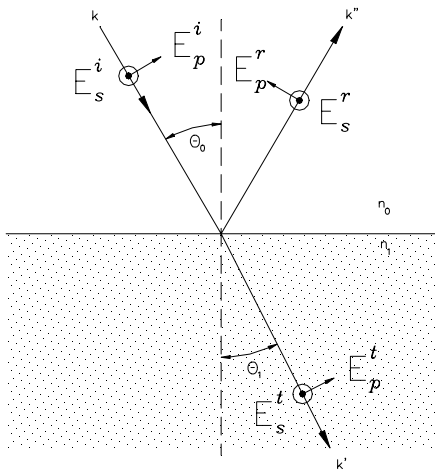


**Figure 2. Specular reflectance ray geometry.** The superscripts “i”, “r”, and “t” stand for incident, reflected, and transmitted, respectively. The subscripts “p” and “s” stand for parallel and perpendicular, respectively. The perpendicular field vectors are out of the paper.

angle, we need to know the number of reflections that the ray makes with the wall and the reflectance at the specified angle. For an angle of propagation,  $\alpha$ , relative to the axis, the effect of a long light guide can be expressed in terms of an effective absorbance equal to

$$A(\alpha) = Na(\alpha),$$

Where

$$N = (L/D)\tan \alpha \quad \text{and}$$

$$a(\alpha) = -\log R_{av}(\alpha).$$

Here,  $L$  = length,  $D$  = diameter, and  $R_{av}(\alpha)$  is the average reflectance at angle  $\alpha$  for all polarization states. The angular reflectances of various materials can be computed if we know the values of the real and imaginary parts of the refractive index. The approach used for this calculation is outlined below.

For this discussion, we will consider a ray of IR radiation incident on a flat surface at an angle of  $\theta_0$  to the normal. In general, this ray will have some state of polarization. The common convention is to resolve the

electric field into components parallel to and perpendicular to the plane of incidence (ie: the plane containing the normal to the surface and the incident ray). These components are called  $E_p$  and  $E_s$  respectively. (Here, “p” stands for “parallel” and “s” stands for the German word “senkrecht”, or perpendicular.) This geometry is illustrated in Figure 2.

In general, the relationships between the incident, reflected, and transmitted electric fields for the two polarization states are given by the Fresnel equations (Ref. 9). For the reflected fields these are:

$$\frac{E_s^r}{E_s^i} = r_s = \frac{n_0 \cos \theta_0 - n_1 \cos \theta_1}{n_0 \cos \theta_0 + n_1 \cos \theta_1}$$

$$\frac{E_p^r}{E_p^i} = r_p = \frac{n_1 \cos \theta_0 - n_0 \cos \theta_1}{n_1 \cos \theta_0 + n_0 \cos \theta_1}$$

Here,  $E_{s,p}^i$  and  $E_{s,p}^r$  are the incident and reflected fields,  $r_s$  and  $r_p$  are the amplitude reflection coefficients for the two polarization states,  $\theta_0$  and  $\theta_1$  are the angles of incidence and refraction, and  $n_0$  and  $n_1$  are the indices of refraction of the two media. In most cases, the first medium will be air ( $n_0 = 1$ ). For the following discussion, we will assume this case and drop the subscript on  $n_1$ .

At first glance, the Fresnel equations look deceptively simple. However, their use is greatly complicated by the fact that the index of refraction is a complex quantity:

$$n = n - ik$$

where the imaginary part,  $k$ , is known as the absorption index. As a result, the angle of refraction and amplitude reflection coefficients are also complex, and the reflectance is given by

$$R_{p,s} = r_{p,s} r_{p,s}^*$$

**Reflectance of Nickel at 10  $\mu\text{m}$  and Glass at 1  $\mu\text{m}$**

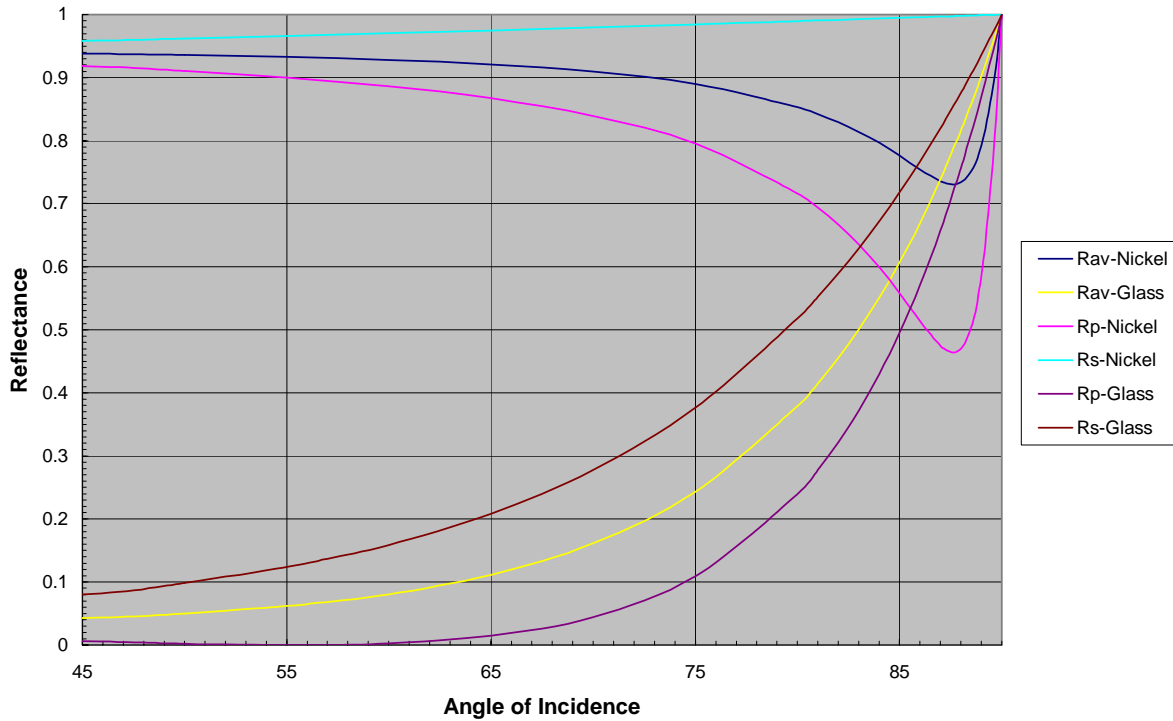


**Figure 3. Reflectance of nickel at 10  $\mu\text{m}$  and borosilicate glass at 1  $\mu\text{m}$  as a function of angle.** “p” state, “s” state and average reflectance are given for each material.

where \* indicates the complex conjugate.

The absorption index is related to the linear absorption coefficient,  $\alpha$ , by the following expression:

$$\alpha = 4\pi\nu k$$

where  $\nu$  is the frequency of the radiation in  $\text{cm}^{-1}$ .

In the general case, it is not possible to write a simple explicit expression for reflectance as a function of angle and polarization state. However, specific values can be obtained by computer solution. To do this, I used the approach of Berning and Berning, outlined in the Handbook of Optics (Ref. 9). Results for a non-absorbing dielectric (borosilicate glass at 1  $\mu\text{m}$ ) and for a typical metal (Nickel at 10  $\mu\text{m}$ ) are given

in Figure 3. As this figure illustrates, the reflectance of each type of material approaches 1.0 as the angle of incidence approaches 90° (grazing). The “p” state reflectance of the metal exhibits a sharp dip at a fairly high incidence angle. This is analogous to the Brewster’s angle (zero reflectance) phenomenon that occurs for the transparent material at a lower incidence angle. As a result, the metal exhibits lower average reflectance than the dielectric for angles very close to grazing. Despite this theoretical advantage of dielectric materials, most of the lightguide systems currently in use employ metallic reflection. This is due to a number of practical considerations including greater strength, ease of machining, and the availability of long lengths of extremely straight metal tubing with excellent surface quality. A further consideration is the marked wavelength

### Reflectance of three metals as a function of angle

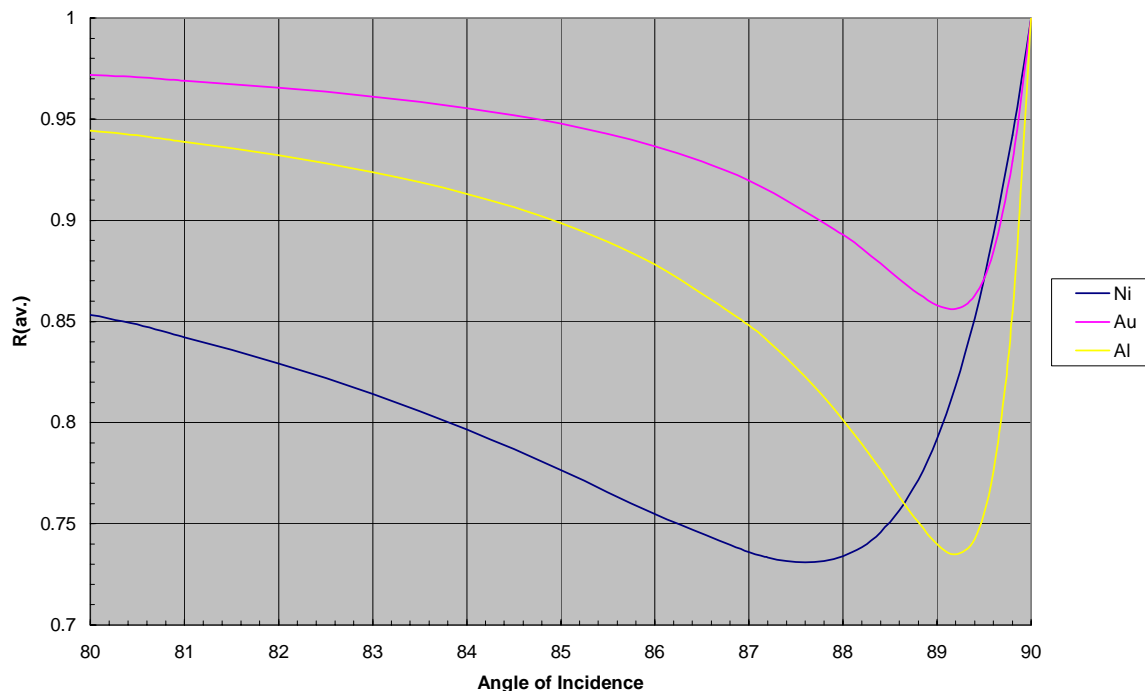


Figure 4. Average reflectance of nickel, gold, and aluminum as a function of angle of incidence.

dependence of the complex refractive index of practical dielectric materials when used in the mid-infrared spectral region.

In predicting the properties of practical lightguides, we are reasonably safe in using the average values of the reflectances for the two polarization states. This is due to the fact that virtually all rays are skew rays to some extent, and given sufficient length, a skew ray will assume all polarization states as it travels through the lightguide. (Ref. 10)

Figure 4 gives the average reflectance of three common metals at angles near grazing. Of these three materials, Nickel and Gold are much more widely used due to their resistance to tarnishing. The choice between these two will depend both on cost and on the anticipated range of incidence angles.

### Predicted Lightguide Transmission Characteristics.

The distribution of ray angles to be encountered in a given idealized lightguide system will be determined by the limiting throughput of the system and the lightguide diameter. In an **FT-IR** based system, the limiting throughput will often be determined either by the interferometer aperture and resolution or by the size of the detector and the numerical aperture of the detector optics. As a typical example, I will assume that the limiting throughput corresponds to a 1 mm diameter detector and 20 mm focal length lens or paraboloid collecting collimated light and focussing it on the detector. In this case, a ray which strikes the edge of the detector will travel at angle of  $1.43^\circ$  to the axis in the collimated region. (See Figure 5.) A typical FT-IR system, will have an

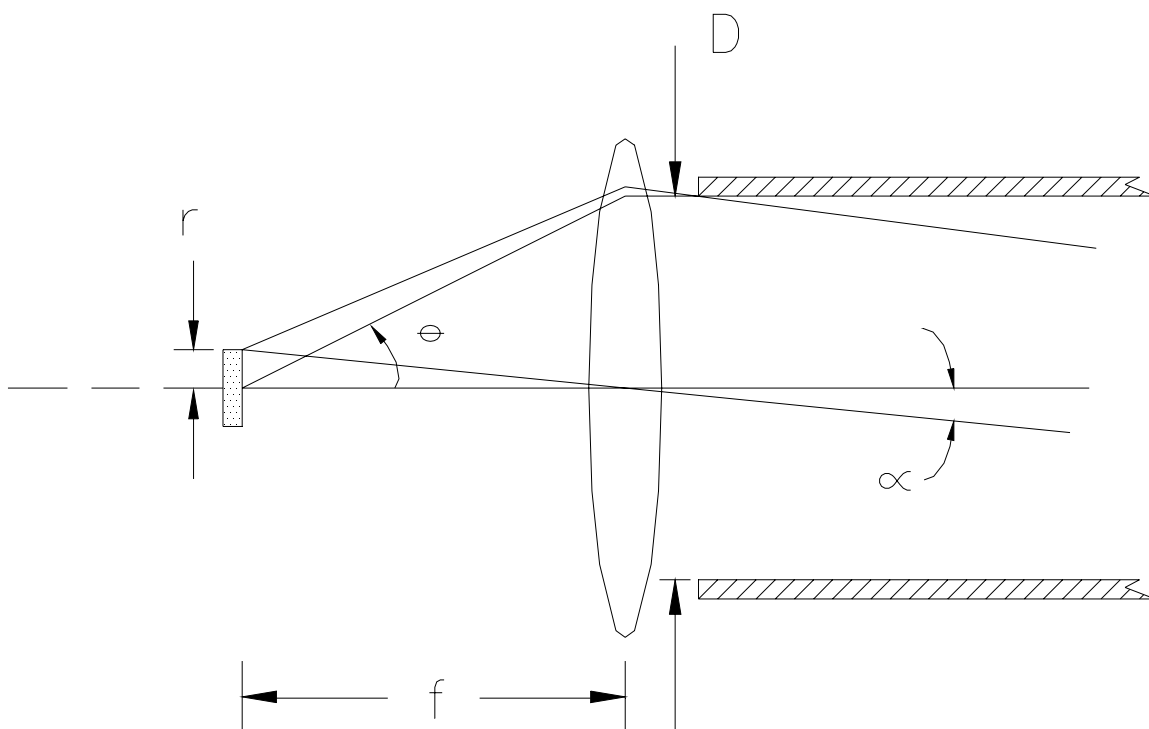


**Figure 5. Idealized detector optical geometry.**

interferometer aperture 32 mm in diameter. This is about the largest diameter collimated beam that can be practically coupled to the assumed detection system. Under this set of conditions, the limiting throughput will correspond to a maximum ray angle of  $1.43^\circ$  passing through a 32-mm diameter aperture.

We will assume that the above FT-IR system is coupled directly to a 32-mm diameter lightguide. To determine the signal transmitted by this lightguide as a function of length, we should, in principle, determine the transmission for each ray in a uniform distribution of ray angles and starting positions and then average these results. As a more convenient and conservative approximation, I will simply assume that all rays are at the maximum divergence angle. Transmission values for the same FT-IR system optimally coupled to other diameter lightguides can then be determined by using the conservation of throughput principle. This, in essence, requires the sine of the maximum ray angle to scale inversely with the lightguide diameter. The results are

given in Figure 6 as a function of lightguide diameter for Nickel and Gold coated light guides. Figure 7 provides the same information as a function of length for the listed lightguide diameters.

The values given in Figures 6 and 7 are convenient “worst case” numbers. Experimentally, for example, we find that 32-mm diameter Ni coated lightguides typically have attenuations in the range of 0.07 absorbance units per meter rather than the value of 0.096 given by Figure 6. We should also note that absorbance is not strictly proportional to pathlength since we actually have a distribution of ray angles. As long as the lightguides are sufficiently straight, this will result a further reduction in incremental absorbance with increased length.

### **Lightguide Based Spectroscopic Immersion Probes.**

In addition to forming the means for transmitting mid-IR radiation between an

## Lightguide Absorbance

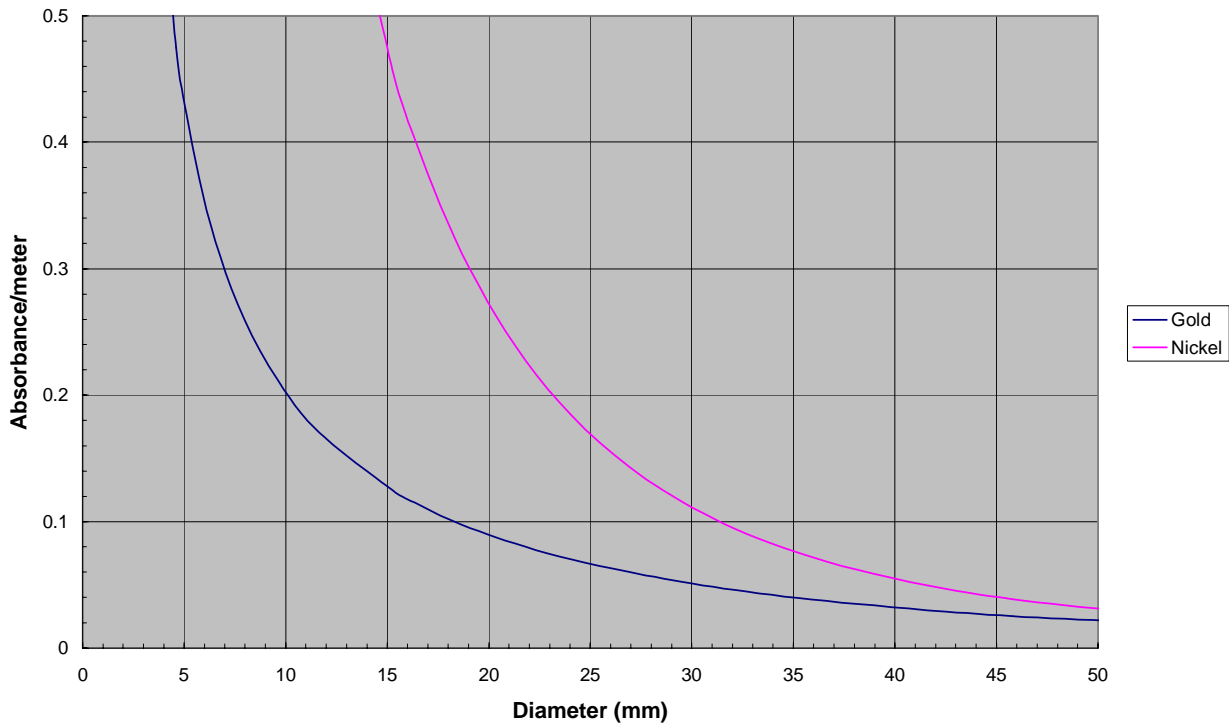


**Figure 6. Worst case absorbance per unit length as function of diameter for gold and nickel lightguides.** The radiation distribution is assumed to be properly matched to each diameter with the limiting throughput corresponding to a uniform distribution of rays with a maximum angle of  $1.43^\circ$  passing through a 32 mm diameter circular aperture.

analyzer and a sampling point, metallic lightguides are critical components in immersion probes for use in both batch reaction vessels and continuous process lines. In the mid-IR spectral region, their use is dictated by the same considerations that apply outside of the reaction vessel – the lack of suitable mid-IR fibers, the need to minimize optics diameter while maximizing transmission, and the need to avoid critical optical tolerances in regions of wide temperature variation or mechanical stress. This third factor is important even when operating in the near-IR or UV-visible regions since the use of optical fibers within a transmission probe necessarily entails collimating or imaging optics in the vicinity of the transmission gap.

Figure 8 illustrates a process mid-IR installation using an attenuated total

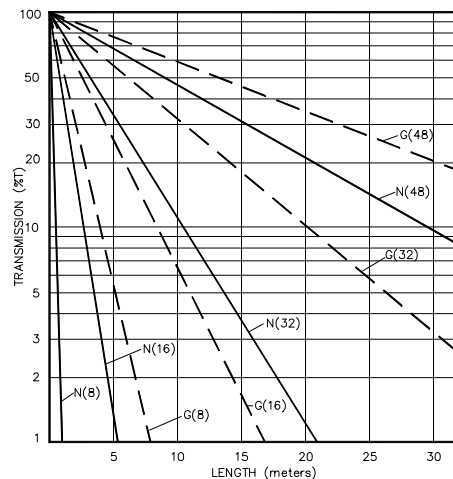


**Figure 7. Transmission versus length for various diameter light guides under the same assumptions as Figure 6.** “G” and “N” refer to gold and nickel respectively. The numbers in parentheses are the light guide inner diameters (mm).

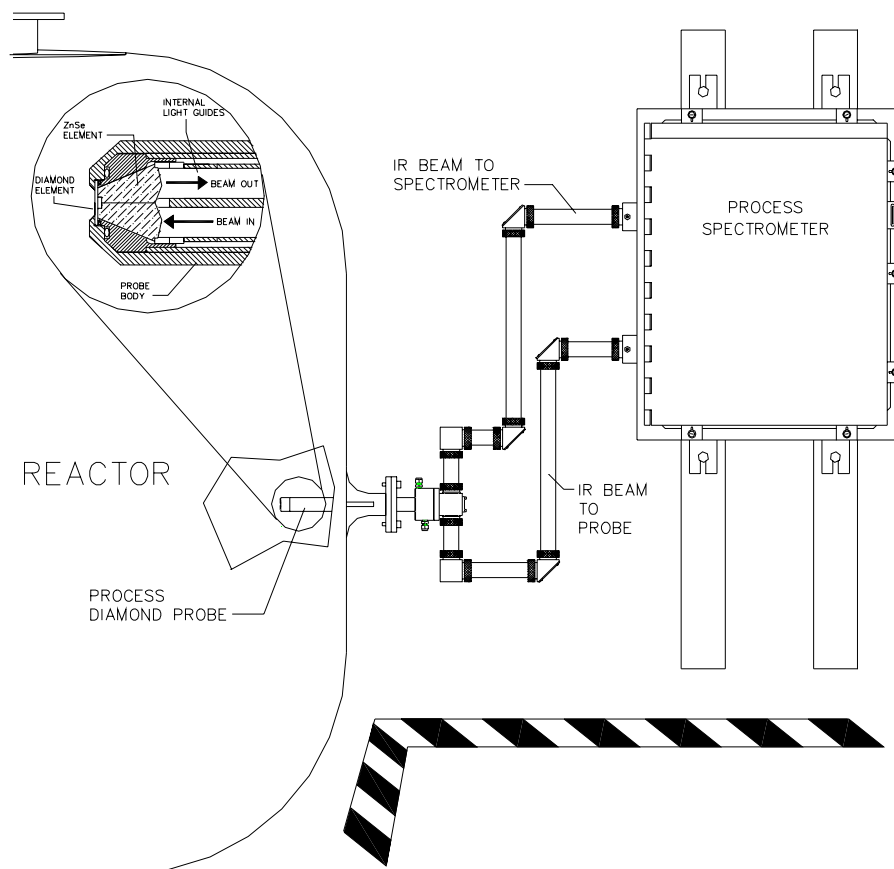


**Figure 8. A mid-infrared process monitoring installation employing a series of hollow metallic lightguides to couple between a diamond-tipped ATR probe and an FTIR spectrometer. Details of the lightguide based probe design are shown in the enlargement.**

reflection (ATR) probe coupled to an FTIR spectrometer by means of a series of hollow light guides and mirror modules. (Refs. 7, 11) This example uses a pair of 8 mm diameter lightguides within the probe to minimize probe diameter and 32 mm diameter lightguides between the probe and the spectrometer for maximum transmission. The ATR element consists of two components with similar refractive indices, which are sandwiched together in intimate optical contact. The first is a flat disk of a material such as diamond or silicon having very high degree of chemical resistance. The second is a complex shaped component fabricated from a more easily worked material such as ZnSe. (Ref. 12) This

provides the appropriate focusing and optical coupling to and from the chemically resistant disk.

In this illustration, the transfer between the two different size lightguides is accomplished by means of a single paraboloid with its focal point located at the entrance of the smaller lightguide. This is an interesting illustration of the conservation of throughput principle. Although the entrance of the smaller lightguide is at the focal point of the paraboloid rather than at the output of a two-element beam condenser, the distribution of rays at this point is the same. This can be understood by realizing that the distribution of radiation in the focal plane

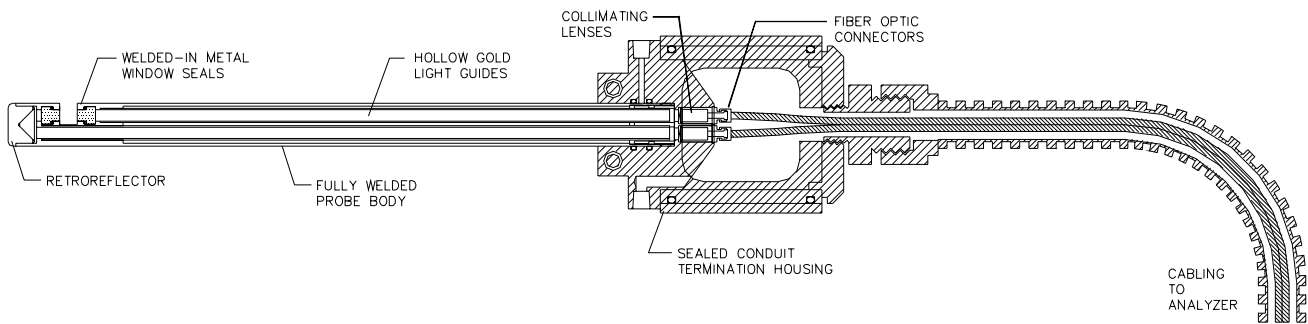


**Figure 9. A lightguide based near-IR transmission probe designed for extreme reliability.** This design employs collimated radiation transmitted through a pair of hollow metallic lightguides in the process-exposed part of the probe so as to provide maximum stability and reliability at extreme temperatures. The radiation is coupled to transmitting and receiving optical fibers by means of a pair of collimators enclosed in a hermetically-sealed conduit termination housing. The exposed parts of the probe are fully welded together, including the metal window seals.

represents the magnified image of either the Lambertian IR source or the IR detector. It thus will have a uniform distribution of ray positions and angles with a throughput equal to the lesser of the detector optics throughput or the interferometer throughput.

A lightguide based near-IR transmission probe is illustrated in Figure 9. In this case, fiber-optic cables are used to transmit radiation to and from the probe. These are terminated at a pair of optical collimators composed of fiber-optic connectors and precisely positioned lenses. Thermal effects are minimized by locating the collimators external to the reaction vessel and surrounding them by a combination conduit termination housing and heat sink. (Ref. 13) Within the probe, the radiation travels through a pair of metallic lightguides, remaining collimated within the transmission gap. The direction of propagation is reversed at the end of the probe by a retro reflector, which can be either a metallic cone or fused silica cube corner. The particular design shown uses fully e-beam welded construction including the retaining of the metal c-ring window seals. (Ref. 12)

### Summary and Conclusion:

Metallic, internally reflecting lightguides – operating with nominally collimated radiation – are widely used both for transmitting mid-IR radiation between an analyzer and an measurement location and as components in both ATR and transmission probes operating in various spectral regions. Compared to imaging-based transmission systems, lightguides have the advantages of simplicity, moderate cost, and a lack of the performance variations which can result from the interaction between optical adjustments and transmission of a lightguide can be maximized by appropriate choice of reflecting material and by providing radiation which is as nearly collimated as possible consistent with the limiting system throughput.

### REFERENCES:

1. W. M. Doyle, Versatile and Efficient Radiation Transmission Apparatus and Method for Spectrometers, U. S. Patent 4,810,093, Mar. 7, 1989.

2. J. Heo, J. S. Sanghera, and J. D. Mackenzie, 'Chalcohalide Glasses For Infrared Fiber Optics', *Opt. Eng.* **30**, 470 (1991).
3. W. M. Doyle, Light Pipe System Having Maximum Radiation Throughput, U. S. Patent 5,054,869, Oct. 8, 1991.
4. O. Morhaim, D. Mendlovic, I. Gannot, J. Dror, and N. Croitoru, 'Ray Model for Transmission of Infrared Radiation Through Multibent Cylindrical Waveguides', *Opt. Eng.* **48**, 531 (1991).
5. M. J. Webb, 'Practical considerations when using fiber optics with spectrometers', *Spectroscopy*, **4** 26 (1989).
6. W. L. Wolf and G. J. Zissis (Eds.), The Infrared Handbook, prepared by the Environmental Research Institute of Michigan for the Office of Naval Research, Washington DC, (1978), p. 20-8.
7. The Axiot System, Data sheet AX-01 (006), Axiom Analytical, Inc., Irvine CA 1990.
8. W. N. Hansen and G. J. Hansen, 'Infrared Spectroscopy of Surface Films and Powders Using a Metal Light Pipe', *Applied Spectroscopy*, **41** 553 (1987).
9. W. G. Driscoll and W. Vaughn (Eds.), Handbook of Optics, McGraw-Hill, New York, 1978, p. 10-7.
10. R. C. Ohlmann, P. L. Richards, and M. Tinkham, 'Far Infrared Transmission through Metal Light Pipes', *J. Opt. Soc. Am.* **48**, 531 (1958).
11. DPR-240 and DMD-370 High Transmission ATR Immersion Probes, Data Sheet PS-DP-01(002), Axiom Analytical, Inc. Irvine CA 2000.
12. W. M. Doyle and N. A. Jennings, 'Spectroscopic Sample Interfacing Under Extreme Process Conditions', Fourteenth International Forum Process Analytical Chemistry, Lake Las Vegas, NV, January 23 – 26, 2000.
13. W. M. Doyle and N. A. Jennings, 'Designing Robust Sample Interfacing Equipment for Infrared Process Analysis', AT-Process, the Journal of Process Analytical Chemistry, Vol. II 366 (1997).